

Organometallic Derivatives of Fullerenes: A DFT Study of $(\eta^2-C_x)\{Pt(PH_3)_2\}_n$ ($x = 60, 70, 84; n = 1-6$)

Josep M. Campanera, Jordi Muñoz, Jordi Vázquez,[†] Carles Bo, and Josep M. Poblet*

Departament de Química Física i Inorgànica, Universitat Rovira i Virgili, Imperial Tàrraco 1, 43005 Tarragona, Spain

Received July 26, 2004

To determine the relationship among curvature, patch type, and reactivity of the C–C site, a series of density functional calculations were performed on several substituted fullerenes. [6:6] pyracylene-type sites are the most reactive sites in all analyzed cages: C_{60} , C_{70} , and C_{84} . The binding energy between the $Pt(PH_3)_2$ unit and fullerene is almost independent of the size of the cage and of the number of metals coordinated on the fullerene surface. Contrarily, curvature and type of carbon–carbon bond are determinant for the coordination strength. The use of relatively large basis sets is necessary to have consistent energies.

Introduction

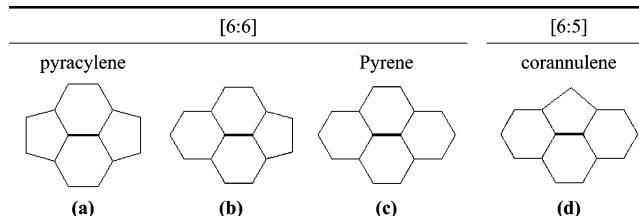
Organometallic derivatives of fullerenes have been synthesized and structurally characterized since the beginning of fullerene coordination chemistry.^{1,2} Addition of the $M(PR_3)_2$ ($M = Pt, Pd, Ni$; $R = Et, Ph$) unit to the most common fullerene, C_{60} , was reported before addition to other fullerenes.^{3,4} With an excess of $M(PEt_3)_4$ the hexaaddition product $(\eta^2-C_{60})\{M(PEt_3)_2\}_6$ ($M = Pt, Pd$) has been obtained.⁵ The monoaddition Vaska-type complexes have also been synthesized and characterized for C_{60} ⁶ and the higher fullerenes C_{70} ⁷ and C_{84} .⁸ Multiple additions are also possible but often lead to a mixture of products. Some double addition

* Author to whom correspondence should be addressed. E-mail: poblet@quimica.urv.es.

[†] Present address: Waste Management Laboratory, Technological Center of Manresa, 08240 Manresa, Spain.

- (1) Hawkins, J. M.; Meyer, A.; Lewis, T. A.; Loren, S.; Hollander, F. J. *Science* **1991**, 252, 312. Hawkins, J. M. *Acc. Chem. Res.* **1992**, 25, 150. Stephens, A. H. H.; Green, M. L. H. *Adv. Inorg. Chem.* **1997**, 44, 1.
- (2) Balch, A. L.; Olmstead, M. M. *Chem. Rev.* **1998**, 98, 2123.
- (3) Fagan, P. J.; Calabrese, J. C.; Malone, B. *Science* **1991**, 252, 1160.
- (4) Lerke, S. A.; Parkinson, B. A.; Evans, D. H.; Fagan, P. J. *J. Am. Chem. Soc.* **1992**, 114, 7807. Bashilov, V. V.; Petrovskii, P. V.; Sokolov, V. I.; Lindeman, S. V.; Guzey, I. A.; Struchkov, Y. T. *Organometallics* **1993**, 12, 991.
- (5) Fagan, P. J.; Calabrese, J. C.; Malone, B. *J. Am. Chem. Soc.* **1991**, 113, 9408. Fagan, P. J.; Calabrese, J. C.; Malone, B. *Acc. Chem. Res.* **1992**, 25, 134.
- (6) Balch, A. L.; Catalano, V. J.; Lee, J. W. *Inorg. Chem.* **1991**, 30, 3980. Vértés, A.; Gál, M.; Wagner, F. E.; Tuczek, F.; Gütllich, P. *Inorg. Chem.* **1993**, 32, 4478.
- (7) Balch, A. L.; Catalano, V. J.; Lee, J. W.; Olmstead, M. M.; Parkin, S. R. *J. Am. Chem. Soc.* **1991**, 113, 8953.
- (8) Balch, A. L.; Ginwalla, A. S.; Noll, B. C.; Olmstead, M. M. *J. Am. Chem. Soc.* **1994**, 116, 2227.

Chart 1. Different Types of C–C Bonds in IPR Fullerenes^a



^aThe [6:6] ring junction is abutted by two pentagons (pyracylene-type site) in (a), by a hexagon and a pentagon in (b), and by two hexagons in (c) (pyrene-type site). The unit in (d) is called a corannulene-type and represents a [6:5] ring junction abutted by two hexagons. The bold lines show the C–C bond considered. In all synthesized complexes of C_{60} , C_{70} , and $D_{2d}(C_{84}:23)$ the metal additions take place at pyracylene-type sites.

products of C_{60} and C_{70} , however, have been well determined: $(\eta^2-C_{60})\{Ir(CO)Cl(PMe_2Ph)_2\}_2$;⁹ $(\eta^2-C_{60})\{Ir(CO)Cl(PR_3)_2\}_2$ ($R = Et, Me$);¹⁰ $(\eta^2-C_{70})\{Ir(CO)Cl(PMe_2Ph)_2\}_2$.¹¹

Although all carbon atoms in C_{60} are chemically equivalent, two different types of C–C bonds can be distinguished corresponding to [6:6] and [6:5] ring junctions (pyracylene- and corannulene-type sites, respectively); see Chart 1. Up now, only metal atoms have been observed attached to the pyracylene [6:6] C–C bonds. One isomer obeys the isolated pentagon rule (IPR) for C_{70} .¹² This structure, which is of

- (9) Balch, A. L.; Lee, J. W.; Noll, B. C.; Olmstead, M. M. *J. Am. Chem. Soc.* **1992**, 114, 10984.
- (10) Balch, A. L.; Lee, J. W.; Noll, B. C.; Olmstead, M. M. *Inorg. Chem.* **1994**, 33, 5238.
- (11) Balch, A. L.; Lee, J. W.; Olmstead, M. M. *Angew. Chem., Int. Ed. Engl.* **1992**, 31, 1356.
- (12) Fowler, P. W.; Manolopoulos, D. E. *An Atlas of Fullerenes*; Oxford University Press: Oxford, U.K., 1995.

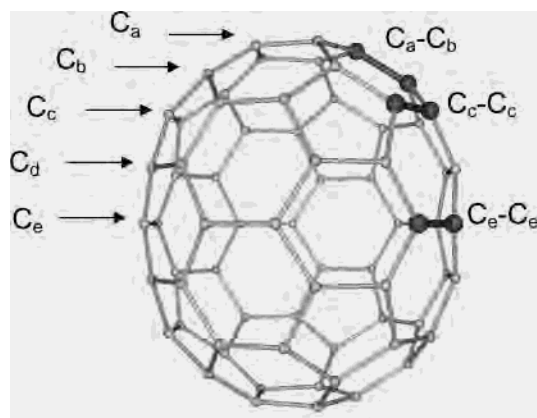


Figure 1. View of different types of carbon bonds and carbon atoms in the free C_{70} . The D_{5h} symmetry of the C_{70} molecule is formed by nine layers of carbons, five types of carbon atoms, and eight distinct C–C bonds. Among the four [6:6] ring junctions, C_a – C_b , C_c – C_c , C_e – C_e , and C_d – C_e , only two are of pyracylene-type sites, C_a – C_b and C_c – C_c . The bold lines show the C–C bonds where $Pt(PH_3)_2$ units are coordinated.

D_{5h} symmetry, has five types of carbon atoms that form nine layers. Connecting these carbon atoms are eight types of C–C bonds, four of which occur at [6:6] ring junctions: C_a – C_b ; C_c – C_c ; C_e – C_e ; C_d – C_e (Figure 1). The first two are pyracylene-type sites while the third is a pyrene-type site (see Chart 1). In the iridium Vaska-type complex $(\eta^2-C_{70})-Ir(CO)Cl(PPh_3)_2$ the C_a – C_b position is preferred.⁷ The reaction of C_{70} with $(\eta^2-C_2H_4)Pt(PPh_3)_2$ leads to the four adducts $(\eta^2-C_{70})\{Pt(PPh_3)_2\}_n$, where $n = 1$ –4. The first two additions take place at the C_a – C_b bonds, at opposite ends of the fullerene, whereas the next two additions occur at the C_c – C_c bonds also at the opposite bonds of the cage.¹³ The structure of C_{84} is more complex and has 24 IPR isomers. Theoretical calculations indicate that isomers 22 and 23 of symmetries D_2 and D_{2d} , respectively, have the lowest energies.¹⁴ The X-ray diffraction of $(\eta^2-C_{84})Ir(CO)Cl(PPh_3)_2$ showed that the geometry of the fullerene portion corresponds to the $D_{2d}-(84:23)$ structure that has 19 different sets of C–C bonds (Figure 2).⁸ Note that all metal additions in the three free fullerenes take place at pyracylene-type sites.

Earlier quantum chemistry calculations at the Hartree–Fock level on complexes of the type $(\eta^2-C_{60})\{M(PH_3)_2\}_n$ with $M = Pd$ or Pt and $n = 1, 2$, or 6 showed that the hemisphere of the C_{60} cage which is furthest from the platinum is essentially unperturbed by the coordination of the metal.^{15,16} Geometries computed for $(\eta^2-C_{60})\{M(PH_3)_2M\}_n$ ($M = Pd, Pt$) ($n = 1, 2, 6$) complexes at HF level are in reasonably good agreement with experimental X-ray data, but the calculated bonding energies between metal and fullerene cage are unreliable at that computational level because the electronic correlation effects are considerable. More recently, Sgamellotti and co-workers analyzed in detail the metal–

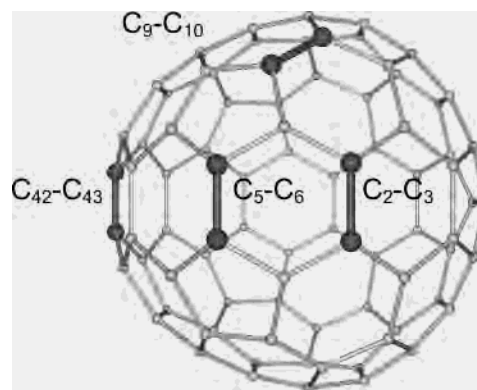


Figure 2. View of different types of carbon bonds in the $D_{2d}-(C_{84}:23)$ isomer with the same atom numbering outlined in ref 34. The bold lines show the C–C bonds where $Pt(PH_3)_2$ units are coordinated.

fullerene bonding in the $(\eta^2-C_{60})M(PH_3)_2$ complexes for $M = Ni, Pd$, and Pt .^{17,18} Since complex formation causes only a local structural deformation of the carbon cage, the pyracylene model for the metal–fullerene interaction has been proposed for C_{60} .¹⁸ To our knowledge no quantum chemistry calculations on organometallic derivatives of higher fullerenes have been reported yet.

The observed structures for these addition products suggest that the curvature of the fullerene enhances significantly the reactivity of the fullerene, facilitating the addition of the different functional group. Accordingly, in C_{70} , the metal is added to the most pyramidalized carbons and in the metal complex the pyramidalization of these atoms increases significantly.¹⁹ The relationship between the local atomic structure and the chemical reactivity of fullerenes was characterized by Haddon using the pyramidalization angle of carbons, θ_p .²⁰

The aim of this article is to evaluate the effect of the fullerene curvature on the metal–fullerene bonding. To this end we have compared the coordination of the $Pt(PH_3)_2$ unit to C_{60} , C_{70} , and C_{84} . We investigated the influence of the multiple addition through the series of polynuclear complexes $(\eta^2-C_{60})\{Pt(PH_3)_2\}_n$ for $n = 2, 4$, and 6.

Theoretical Details

All calculations were carried out using the DFT methodology with the ADF2004 program.²¹ The local spin density approximation characterized by the electron gas exchange was used with Vosko–Wilk–Nusair²² (VWN) parametrization for correlation. Becke²³ and

- (13) Balch, A. L.; Hao, L.; Olmstead, M. M. *Angew. Chem., Int. Ed. Engl.* **1996**, *35*, 188.
 (14) Zhang, B. L.; Wang, C. Z.; Ho, K. M. *J. Chem. Phys.* **1992**, *96*, 7183. Wang, X. Q.; Wang, C. Z.; Zhang, B. L.; Ho, K. M. *Phys. Rev. Lett.* **1992**, *69*, 69. Wang, X. Q.; Wang, C. Z.; Zhang, B. L.; Ho, K. M. *Chem. Phys. Lett.* **1993**, *207*, 349.
 (15) Koga, N.; Morokuma, K. *Chem. Phys. Lett.* **1993**, *202*, 330.
 (16) Bo, C.; Costas, M.; Poblet, J. M. *J. Phys. Chem.* **1995**, *99*, 5914.

- (17) Nunzi, F.; Sgamellotti, A.; Re, N.; Floriani, C. *Organometallics* **2000**, *19*, 1628.
 (18) Nunzi, F.; Sgamellotti, A.; Re, N. *J. Chem. Soc., Dalton Trans.* **2002**, 399.
 (19) Haddon, R. C. *Science* **1993**, *261*, 1545.
 (20) Haddon, R. C.; Scott, L. T. *Pure Appl. Chem.* **1986**, *58*, 137. Haddon, R. C. *J. Am. Chem. Soc.* **1986**, *108*, 2837. Haddon, R. C. *Acc. Chem. Res.* **1988**, *21*, 243. Haddon, R. C. *J. Am. Chem. Soc.* **1990**, *112*, 3385. Haddon, R. C.; Chow, S. Y. *J. Am. Chem. Soc.* **1998**, *120*, 10494.
 (21) *ADF2004.01*; SCM, Theoretical Chemistry, Vrije Universiteit: Amsterdam, The Netherlands, <http://www.scm.com>. te Velde, G.; Bickelhaupt, F. M.; Gisbergen, S. J. A. van; Fonseca Guerra, C.; Baerends, E. J.; Snijders, J. G.; Ziegler, T. Chemistry with ADF. *J. Comput. Chem.* **2001**, *22*, 931. Fonseca Guerra, C.; Snijders, J. G.; te Velde, G.; Baerends, E. J. *Theor. Chem. Acc.* **1998**, *99*, 391.
 (22) Vosko, S. H.; Wilk, L.; Nusair, M. *Can. J. Phys.* **1980**, *58*, 1200.
 (23) Becke, A. D. *J. Chem. Phys.* **1986**, *84*, 4524; *Phys. Rev.* **1988**, *A38*, 3098.

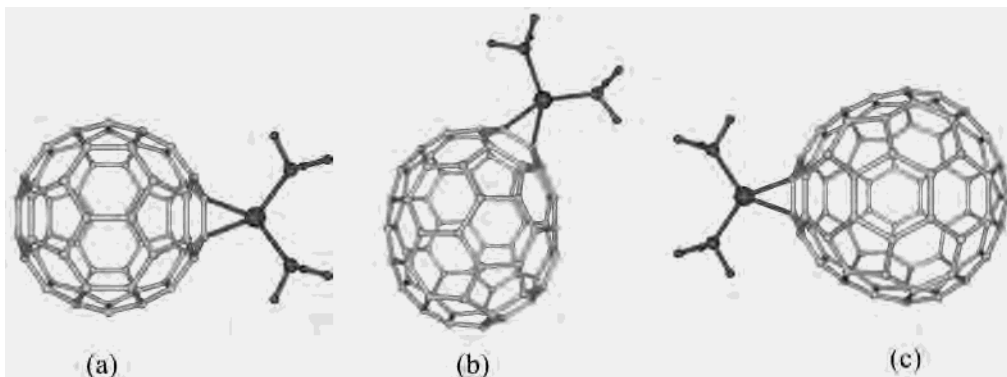


Figure 3. Structure of the most stable isomers of $(\eta^2-C_{60})Pt(PH_3)_2$, with a metal unit link to [6:6] ring junction (a), $(\eta^2-C_{70})Pt(PH_3)_2$, with a metal unit link to C_a-C_b (b), and $(\eta^2-C_{84})Pt(PH_3)_2$, with a metal unit link to $C_{42}-C_{43}$ (c).

Table 1. DFT Geometries and Binding Energies (BE) for the $(\eta^2-C_{60})Pt(PH_3)_2$, $(\eta^2-C_{14}H_8)Pt(PH_3)_2$, and $(\eta^2-C_2H_4)Pt(PH_3)_2$ Model Clusters^a

molecule	method	basis set	Pt–P	Pt–C	C–C	P–Pt–P	BE ^b	BSSE ^c	ref
$(\eta^2-C_{60})Pt(PH_3)_2$	X-ray		2.278	2.130	1.502	102.4			3
$(\eta^2-C_{60})Pt(PH_3)_2$	DFT	TZP	2.297	2.139	1.495	106.3	–22.2	1.2	this study
		C (DZP); C patch, P, H, Pt (TZP)	2.293	2.120	1.504	105.4	–24.6	2.1	this study
		C (DZP); P, H, Pt (TZP)	2.297	2.137	1.495	106.3	–32.6	8.4	this study
		TZP	2.271	2.065	1.528	116.0	–28.0	1.9	18
$(\eta^2-C_{14}H_8)Pt(PH_3)_2$	DFT	C, P, H (DZP); Pt (TZP)	2.277	2.112	1.503	117.3	–22.0	6.7	18
		TZP	2.294	2.148	1.432	106.4	–20.6	0.5	this study
$(\eta^2-C_2H_4)Pt(PH_3)_2$	DFT	C, H ethylene (DZP); Pt, P, H (TZP)	2.294	2.147	1.431	106.4	–21.2	2.3	this study

^a Bond lengths in Å, angles in deg, and energies in kcal mol^{–1}. ^b The binding energies (BE) between the fullerene and M(PH₃)₂ fragments have been calculated according to the following scheme: M(PH₃)₂ + C₆₀ → $(\eta^2-C_{60})Pt(PH_3)_2$. Dissociation energy (DE) is equal to –BE. The BE do not include BSSE corrections. ^c Basis set superposition error (BSSE).

Perdew²⁴ nonlocal corrections were added to the exchange and correlation energy, respectively. In most calculations, we used a basis set composed of triple- ζ + polarization (TZP) Slater basis sets for the valence electrons of all atoms. A frozen core consisting of the 1s and 1s–2p shells was described by means of single Slater functions for C and P, respectively. For platinum atoms, the inner electrons 1s–4spd were considered frozen and described by means of single Slater functions, the 5s and 5p electrons by double- ζ Slater functions, the 5d and 6s by triple- ζ functions, and the 6p by a single orbital.²⁵ The ZORA formalism²⁶ with corrected core potentials was used to make quasirelativistic corrections for the core electrons. The quasirelativistic frozen core shells were generated with the auxiliary program DIRAC.²¹ Additional calculations were carried out with double- ζ + polarization (DZP) Slater basis sets for valence electrons of atoms of the ligand unit (fullerene cage/ethylene) and TZP basis set for the remaining Pt, P, and H atoms of the Pt(PH₃)₂ unit. Pyramidalization angles (θ_p) have been calculated using the π -orbital axis vector approach (POAV1)²⁰ as implemented in the MOL2MOL program.²⁷

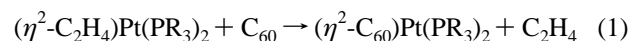
Results and Discussion

C₆₀. The geometries of the $(\eta^2-C_{60})Pt(PH_3)_2$ complex, the free C₆₀, and the Pt(PH₃)₂ unit were computed first with a TZP basis set for all atoms under the constraints of C_{2v}, I_h,

and C_{2v} symmetry groups, respectively. The bond distances found for C₆₀ were 1.397 Å for [6:6] C–C bond and 1.452 Å for [6:5], which were very close to the experimental parameters 1.401 and 1.458 Å.²⁸ The addition of a Pt(PH₃)₂ unit to C₆₀ in a [6:6] C–C bond generated a certain distortion in the fullerene cage, mainly in the interacting region (see Figure 3a). As a result, the coordinated C–C bond increased to 1.495 Å in the complex. This computed distance only slightly differs with the X-ray value reported for $(\eta^2-C_{60})Pt(PH_3)_2$,³ 1.502 Å. The deviations of the computed Pt–P and Pt–C bond lengths from the experimental values are also very small as Table 1 shows.

The dissociation energy (DE) of $(\eta^2-C_{60})Pt(PH_3)_2$ to give the fullerene and the metal unit was computed to be 22.2 kcal mol^{–1}, a relatively high energy that stresses the stability of the organometallic derivatives of C₆₀. The hypothetical isomer with the metal linked to a [6:5] C–C bond was also studied. This isomer is 11.8 kcal mol^{–1} less stable than the observed cluster with the metal atom bonded to a [6:6] C–C bond. In agreement with the lower metal–cage interaction in the [6:5] metal addition, the Pt–C bond distance in this isomer is 0.042 Å longer than in the [6:6] complex and the P–Pt–P angle is somewhat greater: 112.5 and 106.3° in the [6:5] and [6:6] complexes, respectively.

The monosubstituted complex $(\eta^2-C_{60})Pt(PR_3)_2$ is prepared through the substitution reaction



- (24) Perdew, J. P. *Phys. Rev.* **1986**, *84*, 4524; **1986**, *B34*, 7406.
 (25) Snijders, J. G.; Baerends, E. J.; Vernooijs, P. *At. Nucl. Data Tables* **1982**, *26*, 483. Vernooijs, P.; Snijders, J. G.; Baerends, E. J. *Slater type basis functions for the whole periodic system*; Internal Report; Free University of Amsterdam: The Netherlands, 1981.
 (26) Lenthe, E. van; Baerends, E. J.; Snijders, J. G. *J. Chem. Phys.* **1993**, *99*, 4597. Lenthe, E. van; Baerends, E. J.; Snijders, J. G. *J. Chem. Phys.* **1994**, *101*, 9783. Lenthe, E. van; Ehlers, A. E.; Baerends, E. J. *J. Chem. Phys.* **1999**, *110*, 8943.
 (27) Gunda, T. E. *Mol2Mol version 4.0*; CompuChem Software Chemie: Niedernhall, Germany, 2001.

- (28) Hedberg, K.; Hedberg, L.; Bethune, D. S.; Brown, C. A.; Dorn, H. C.; Johnson, R. D.; de Vries, M. *Science* **1991**, *254*, 410.

Reaction 1 is exothermic by only 1.6 kcal mol⁻¹ with a TZP for all atoms. So, whereas the DE for the fullerene complex is 22.2 kcal mol⁻¹, almost the same dissociation energy is found for the ethylene complex at this level of computation, 20.6 kcal mol⁻¹. This difference seems very small, and in fact the energy of the ethylene dissociation has been reported to be 28.2 kcal mol⁻¹ at the CCSD(T) level²⁹ and 22.8 kcal mol⁻¹ at the NL-DFT+QR level.³⁰ Moreover, there remains some discrepancy with the experiment calorimetric studies for (η^2 -C₂H₄)Pt(PPh₃)₂ which leads to an estimate of 36 ± 4 kcal mol⁻¹ for the Pt–C₂H₄ bond energy.³¹ Rosa et al. have shown that the basis set superposition errors (BSSE) are very small when these larger basis sets are used. In transition metal complexes when TZP basis set are used the BSSE has been estimated to be typically between 1 and 2 kcal mol⁻¹,³² and therefore, this correction at this level of computation can be neglected. The calculated BSSE was also found in this order of magnitude for our complexes using TZP: 1.2 kcal mol⁻¹ for (η^2 -C₆₀)Pt(PH₃)₂; 0.5 kcal mol⁻¹ for (η^2 -C₂H₄)Pt(PH₃)₂. All geometries and BE values for the above-mentioned exohedral metallofullerenes are collated in Table 1. Notice that all binding energies (BE) do not include BSSE corrections but this term is listed near the BE values.

With the perspective of studying larger fullerene–metal systems than those reported herein, we have analyzed the effect of the basis on the dissociation energies and geometries. If the C₆₀ is described by a DZP basis set and the Pt moiety by a TZP, the geometry hardly changes but the DE increases up to 32.6 kcal mol⁻¹, whereas the corresponding value for ethylene precursor is 21.2 kcal mol⁻¹. Moreover, higher BSSE corrections are calculated when the DZP basis set is used for the ligand (fullerene/ethylene): 8.4 kcal mol⁻¹ for fullerene; 2.3 kcal mol⁻¹ for ethylene. The discrepancy observed in the dissociation energy motivated us to check a mixed basis set for the carbon cage. That is, the reactant pyracylene unit is described by a TZP and the rest of the carbon cage by a DZP. In these conditions, the X-ray geometry is well reproduced (Table 1) and the DE is now computed as 24.6 kcal mol⁻¹, only 2.4 kcal mol⁻¹ higher than that found with the largest TZP basis set; the BSSE correction is also quite small, 2.1 kcal mol⁻¹. It should also be pointed out that the energies of the frontier orbitals are very similar to those found with the TZP basis: with the mixed basis, the HOMO and LUMO energies are –5.97 and –4.64 eV, while the corresponding values with the largest basis set are –5.54 and –4.16 eV, respectively. This latter point is very important for describing the chemical properties of the complex.

An alternative process has been proposed by Sgamellotti and co-workers.¹⁸ They have used a pyracylene unit as model

(29) Dedieu, A. *Chem. Rev.* **2000**, *100*, 543. Frenking, G.; Antes, I.; Böhme, M.; Dapprich, S.; Ehlers, A. W.; Jonas, V.; Neuhaus, A.; Otto, M.; Stegmann, R.; Veldkamp, A.; Vyboishchikov, S. F. In *Reviews in Computational Chemistry*; Lipkowitz, K. B., Boyd, D. B., Eds.; VCH Publishers: New York, 1996; Vol. 8, p 63.

(30) Ziegler, T.; Tschinke, V.; Baerends, E. J.; Snijders, J. G.; Ravenek, W. *J. Phys. Chem.* **1989**, *93*, 3050.

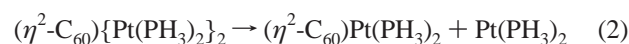
(31) Mortimer, C. T. *Rev. Inorg. Chem.* **1984**, *6*, 233.

(32) Rosa, A.; Ehlers, A. W.; Baerends, E. J.; Snijders, J. G.; te Velde, G. *J. Phys. Chem.* **1996**, *100*, 5690.

for the C₆₀ cage in (η^2 -C₆₀)Pt(PH₃)₂ to reduce the size of the system. When a DZP basis set is used for carbon, phosphorus, and hydrogen and a TZP basis set is used for platinum, the DE for (η^2 -C₁₄H₈)Pt(PH₃)₂ is 22.0 kcal mol⁻¹ but with a large BSSE of 6.7 kcal mol⁻¹, although if a TZP basis set is used to describe all atoms the DE becomes 28.0 kcal mol⁻¹ with a BSSE of 1.9 kcal mol⁻¹.¹⁸ However, the geometry of the monoaddition complex is not properly reproduced even if this larger basis set is used: the angle P–Pt–P is always overestimated and the Pt–C bond length is predicted to be 0.065 Å shorter.

To analyze how the multiple addition affects the binding energy, the series of complexes (η^2 -C₆₀){Pt(PH₃)₂}_n with n = 2, 4, and 6 were fully optimized. Several years ago, we demonstrated that the interaction is quite local and that the loss of the first platinum group in (η^2 -C₆₀){Pt(PH₃)₂}₂ is only slightly more favorable than the loss of the platinum group from the monosubstituted derivative. The calculations that were carried out at the Hartree–Fock level, however, gave very low absolute energies (10.2 kcal mol⁻¹ for the monoadduct). To check these results, we reanalyzed at the DFT level the series of complexes above-mentioned with the largest basis set, TZP for all atoms. Again, the optimized geometries at the present DFT level are in excellent agreement with the X-ray data available. For example, for the hexasubstituted complex, in which the platinum atoms are arranged in an octahedral array around the fullerene core, the computed C–C bond length is 1.487 Å while the X-ray value is 1.497 Å for (η^2 -C₆₀){Pt(PEt₃)₂}₆.⁵ This good agreement is also confirmed in the Pt–P and Pt–C bonds where the deviations are ~0.04 Å. The deviations found at the HF level were a bit more important (~0.05 Å).¹⁶ The Pt–C distances slightly increase as the number of metals on the surface increases. Thus, the Pt–C bond length is 2.139 Å for the monoadduct and 2.153 Å when n = 6. The pyramidalization angle (θ_p) of the carbon atoms coordinated to the metal augments and the maximum distortion appears in the monoaddition complex. When metals are successively added to the fullerene core, the pyramidalization angle of the substituted carbons decreases (Table 2).

The present DFT calculations fully confirm that the addition of one metal group to the C₆₀ only slightly reduces the ability of the carbon cluster to accept a second metal. The reaction energy for the process



is found to be 18.3 kcal mol⁻¹, which is only 3.9 kcal mol⁻¹ smaller than for the dissociation energy of the monosubstituted complex. Thus, the binding energy (BE) per group is –20.3 kcal mol⁻¹ for n = 2. Because of the pentacoordinated complex's low symmetry, the energy associated with the loss of the first metal group in the hexaadduct complex was not determined. Nevertheless, we computed the reaction energy for the process

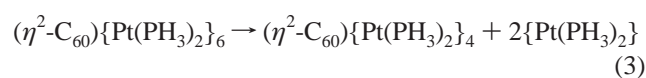


Table 2. Selected Parameters and Metal–Fullerene Binding Energies (BE) for (η^2 -C₆₀){Pt(PH₃)₂}_n Complexes^a

n	patch type	sym	Pt–P	Pt–C	$\Delta(C-C)^b$	P–Pt–P	θ_p^c	BE ^d	BE/group ^e	BSSE ^f
1	corannulene	C _s	2.293	2.181	0.078	112.5	15.47	–10.4	–10.4	1.6
1	pyracylene	C _{2v}	2.297	2.139	0.098	106.3	15.36	–22.2	–22.2	1.2
2	pyracylene	D _{2h}	2.289	2.131	0.103	108.2	15.36	–18.3	–20.3	1.1
4	pyracylene	D _{2h}	2.288	2.150	0.094	107.7	15.07	–18.8	–19.6	1.4
6	pyracylene	T _h	2.289	2.153	0.090	108.1	14.88	–16.7	–18.6	1.1

^a Bond lengths in Å, angles in deg, and energies in kcal mol^{–1}. ^b Difference between the original bond in the free C₆₀ and in the complex. ^c Pyramidalization angle (θ_p) for the carbon atoms attached to metal. θ_p for the free C₆₀ is equal to 11.67°. ^d BE from the previous coordination, so it computes the reaction energy of the (η^2 -C₆₀){Pt(PH₃)₂}_{n–1} + Pt(PH₃)₂ → (η^2 -C₆₀){Pt(PH₃)₂}_n process. For $n = 4$ and $n = 6$ the BE is estimated from the reaction energies (η^2 -C₆₀){Pt(PH₃)₂}_{n–2} + 2{Pt(PH₃)₂} → (η^2 -C₆₀){Pt(PH₃)₂}_n and the tendency observed from $n = 2$ to $n = 1$. ^e The BE/group is calculated from the reaction energy (ΔE) for C₆₀ + n {Pt(PH₃)₂} → (η^2 -C₆₀){Pt(PH₃)₂}_n; BE/group = $\Delta E/n$; ΔE , reaction energy. BE/group does not include BSSE corrections. ^f BSSE of BE/group.

Table 3. Optimized Geometries and Binding Energies (BE) for (η^2 -C₇₀)Pt(PH₃)₂ and (η^2 -C₈₄)Pt(PH₃)₂^a

fullerene cage	site ^b	patch type	sym	Pt–P	Pt–C	$\Delta(C-C)^c$	θ_p free ^d	θ_p^d	BE ^e	BSSE
C ₇₀	C _a –C _b	pyracylene	C _s	2.306	2.140	0.104	11.92	15.66	–24.1	1.3
	C _c –C _c	pyracylene	C _s	2.277	2.142	0.097	11.49	15.25	–21.9	1.2
	C _e –C _e	pyrene	C _{2v}	2.305	2.183	0.115	8.60	12.69	–5.0	1.1
D _{2d} -(C ₈₄ :23)	C ₄₂ –C ₄₃	pyracylene	C _{2v}	2.218	2.175	0.088	10.80	14.35	–23.2	2.1
	C ₉ –C ₁₀	pyracylene	C ₂	2.234	2.152	0.079	10.68	14.34	–21.0	1.8
	C ₅ –C ₆	pyracylene	C _s	2.305	2.163	0.076	10.98	14.53	–19.2	1.9
	C ₂ –C ₃	pyrene	C _s	2.289	2.165	0.098	7.67	11.94	–7.6	1.8

^a Bond lengths in Å, angles in deg, and energies in kcal mol^{–1}. ^b C–C bond linked to the metal (see Figure 1 for C₇₀ and Figure 2 for C₈₄). ^c Difference between the bond distance in the free fullerene and in the complex. For the free C₇₀: C_a–C_b, 1.398 Å; C_c–C_c, 1.392 Å; C_e–C_e, 1.469 Å. For the free D_{2d}-(C₈₄:23) fullerene: C₄₂–C₄₃, 1.375 Å; C₉–C₁₀, 1.369 Å; C₅–C₆, 1.377 Å; C₂–C₃, 1.461 Å. ^d Pyramidalization angle for the coordinated C–C bond in the free fullerene and in the complex. ^e BE does not include BSSE corrections.

which is 33.5 kcal mol^{–1}. The tendency of the dissociation energy when going from $n = 1$ to $n = 2$ suggests that the loss of the first metal group in (η^2 -C₆₀){Pt(PH₃)₂}₆ should be almost ~ 14.8 kcal mol^{–1} (C₆₀M₆ → C₆₀M₅ for short), whereas the dissociation process from C₆₀M₅ to C₆₀M₄ is estimated to be ~ 18.7 kcal mol^{–1}. The same strategy was followed for $n = 4$ and $n = 3$. The energy involved in the C₆₀M₄ → C₆₀M₂ process is equal to 37.7 kcal mol^{–1}, which yields estimated values of ~ 16.9 and ~ 20.8 kcal mol^{–1} for C₆₀M₄ → C₆₀M₃ and C₆₀M₃ → C₆₀M₂, respectively. All these energies are clearly larger than the energy involved in the coordination of a platinum atom to a [6:5] ring junction (10.4 kcal mol^{–1}). Consequently, the metal addition always takes place at the [6:6] C–C bond. To remove the six groups from the fullerene surface requires 111.7 kcal mol^{–1}, a considerable amount of energy that shows how stable these highly substituted fullerenes are. The BE/group in the complexes (η^2 -C₆₀){Pt(PH₃)₂}_n range from –22.2 for $n = 1$ to –18.6 for $n = 6$. The maximum number of metal groups coordinated to the C₆₀ is probably imposed by the steric effects of the bulky PEt₃ ligands.

C₇₀ and C₈₄. By analyzing the (η^2 -C₇₀)Pt(PH₃)₂ and (η^2 -C₈₄)Pt(PH₃)₂ complexes, we have been able to evaluate the importance of the fullerene curvature and the different nature of the carbon atoms in the bonding between the metal and the fullerene cage. C₇₀ and C₈₄ are less spherical than C₆₀, and their cages have carbon atoms with different pyramidalization angles. The curvature of these higher fullerenes is different on each part of the fullerene's surface.

The C₇₀ is most curved at the poles and flatter at the equator. The C_e carbons at the equator of the molecule are the least pyramidalized with $\theta_p = 8.60^\circ$, whereas the C_a and C_b carbons at the poles have the highest pyramidalization angle, 11.92°. The pyramidalization of the other carbon atoms

is between these values. To determine the dependence of the metal–carbon binding energy on the fullerene curvature, we studied the coordination of the Pt(PH₃)₂ unit to the C_e–C_e, C_c–C_c, and C_a–C_b bonds (Figure 1). As in C₆₀, the computed and experimental³³ geometries for the free C₇₀ are in excellent agreement. The computed bond lengths of the pyracylene C_c–C_c and C_a–C_b bonds, 1.392 and 1.398 Å (see Table 3), respectively, are similar to those of the [6:6] C–C bonds in C₆₀. The C_e–C_e bond of 1.469 Å corresponds to a [6:6] ring junction abutted by two hexagons, corresponding to a pyrene-type site. According to a Hückel analysis the π -bond order follows the same trend as pyramidalization. The highest orders are in the poles, C_a–C_b and C_c–C_c bonds, while the equator is more aromatic with low π -bond order in the C_e–C_e bond.³⁴

When a Pt(PH₃)₂ unit is linked to the C_a–C_b bond, the deformation of the fullerene cage and the geometry of the Pt(PH₃)₂ unit is similar to that observed in the C₆₀ derivative (see Tables 2 and 3). The structure of this complex is given in Figure 3b. In consonance with this similarity in the geometries, both complexes differ in the binding energy to give the fullerene cage and the metal unit in only 1.9 kcal mol^{–1} more favorable to C₇₀ addition. When a metal coordinates the fullerene through the C_c–C_c bond, the complex is somewhat less stable and the BE is –21.9 kcal mol^{–1}, 2.2 kcal mol^{–1} lower than for the most stable isomer. The dissociation energy for the complex in which the metal is linked to the carbons at the equator is only 5.0 kcal mol^{–1}. This lower energy is because of the different nature of the [6:6] C_e–C_e bonds (pyrene-type sites) and the smaller pyramidalization angle of the C_e carbons. Note that this later

(33) Hedberg, K.; Hedberg, L.; Bühl, M.; Bethune, D. S.; Brown, C. A.; Dorn, H. C.; Johnson, R. D. *J. Am. Chem. Soc.* **1997**, *119*, 5314.

(34) Taylor, R. *J. Chem. Soc., Perkin Trans. 2* **1993**, 813.

Table 4. Description of the 19 Different C–C Bonds of the D_{2d} -(C₈₄:23) Fullerene

C–C bond ^a	ring junction	patch type ^b	bond length	θ_p ^c	π bond order ^d
5,6	[6:6]	pyracylene (a)	1.377	10.98	0.593
42,43	[6:6]	pyracylene (a)	1.375	10.80	0.624
9,10	[6:6]	pyracylene (a)	1.369	10.68	0.611
7,22	[6:6]	b	1.416	9.68	0.553
21,41	[6:6]	b	1.423	9.67	0.535
1,2	[6:6]	b	1.419	9.32	0.572
11,12	[6:6]	b	1.427	9.30	0.540
12,13	[6:6]	b	1.413	8.80	0.548
21,22	[6:6]	pyrene (c)	1.468	8.73	0.489
2,12	[6:6]	pyrene (c)	1.465	7.78	0.489
2,3	[6:6]	pyrene (c)	1.461	7.67	0.509
1,6	[6:5]	corannulene (d)	1.431	10.97	0.507
1,9	[6:5]	corannulene (d)	1.445	10.83	0.471
5,20	[6:5]	corannulene (d)	1.453	10.81	0.451
23,43	[6:5]	corannulene (d)	1.446	10.71	0.557
8,9	[6:5]	corannulene (d)	1.444	10.70	0.466
7,8	[6:5]	corannulene (d)	1.428	10.67	0.541
13,31	[6:5]	corannulene (d)	1.424	10.16	0.558
13,14	[6:5]	corannulene (d)	1.456	9.71	0.435

^a Systematic numeric system from ref 34. ^b See Chart 1 for a schematic representation of the different motifs: pyracylene (a), b, pyrene (c), and corannulene (d). ^c Average pyramidalization angle of each carbon atom in the carbon bond. ^d Reference 34.

energy is even smaller than that found for the C₆₀ derivative with the metal coordinated to the [6:5] C–C bond. The relatively short Pt–C bond lengths, 2.183 Å, do not reveal the significant instability of the isomer with the metal bonded to a C_e–C_e bond.

Balch and co-workers have shown that the addition of Ir(CO)Cl(PPh₃)₂ to a benzene solution of a mixture of C₈₄ isomers yields the (η^2 -C₈₄)Ir(CO)Cl(PPh₃)₂ complex.⁸ The X-ray analysis of this system showed that the fullerene cage correspond to the D_{2d} -(84:23) isomer. According to the Taylor numeration, the coordination of the iridium atom takes place at the C₄₂–C₄₃³⁵ bond, one of the three distinct pyracylene-type sites (C₅–C₆, C₉–C₁₀, and C₄₂–C₄₃; see Figure 2). These three bonds have the shortest C–C distances (~1.37 Å) and the highest pyramidalized carbon atoms of the [6:6] sites ($\theta_p \approx 11.0^\circ$). Moreover, according to Hückel calculations the pyracylene carbon–carbon bonds have the highest π -bond order. So, in accordance with these criteria, the pyracylene sites should be the most reactive. On the other hand, the pyrene units contain the longest [6:6] C–C bonds (~1.46 Å) and the corresponding carbon atoms have small pyramidalization angles (~8°). These geometrical parameters suggest that pyrene sites should be the least reactive of the [6:6] sites. Table 4 describes the 19 distinct C–C bonds for the D_{2d} -(84:23) isomer. To evaluate the strength of the fullerene–metal bond we studied the coordination of the Pt(PH₃)₂ unit to the three [6:6] pyracylene C–C bonds and to the C₂–C₃ bond, one of the three pyrene-type sites. The addition to the latter will allow us to establish an energy range for the [6:6] C–C bonds. The energy values in Table 3 fully confirm that the most reactive site corresponds to C₄₂–C₄₃, the coordination position observed by Balch in the (η^2 -C₈₄)Ir(CO)Cl(PPh₃)₂ Vaska-type complex. The binding energy of –23.2 kcal mol^{–1} is only somewhat lower than that found at the same level of computation the most reactive

(35) Notice that Ir links to the C₃₂–C₅₃ bond in ref 8 but this C–C bond is equivalent also to C₄₂–C₄₃ bond according to numbering scheme proposed by Taylor for D_{2d} -(84:23) in ref 34.

Table 5. Mulliken Net Charges for Several Fullerenes Coordinate to Pt(PH₃)₂

fullerene cage	site ^a	metal no.	C ₂ ^b	Pt	Pt(PH ₃) ₂ ^c
C ₆₀	[6:5]	1	–0.632	0.292	0.614
	[6:6]	1	–0.656	0.330	0.688
	[6:6] ^d	2	–0.688	0.327	0.649
	[6:6] ^d	4	–0.676	0.294	0.559
C ₇₀	[6:6] ^d	6	–0.670	0.281	0.512
	C _a –C _b	1	–0.676	0.326	0.698
	C _c –C _c	1	–0.646	0.336	0.689
	C _e –C _e	1	–0.662	0.243	0.561
C ₈₄	C ₄₂ –C ₄₃	1	–0.589	0.312	0.664
	C ₉ –C ₁₀	1	–0.604	0.330	0.659
	C ₅ –C ₆	1	–0.590	0.265	0.627
	C ₂ –C ₃	1	–0.730	0.257	0.576

^a C–C bond linked to the metal (see Figure 1 for C₇₀ and Figure 2 for D_{2d} -(C₈₄:23)). ^b Net charge for the C₂ unit coordinated to the metal. ^c Net charges for the Pt(PH₃)₂ unit. ^d Average values.

site in the C₇₀ and only a bit higher for the C₆₀. The structure of the metal complex linked to the C₄₂–C₄₃ bond is given in Figure 3c. The BE energy computed for the other two pyracylene positions (C₅–C₆ and C₉–C₁₀) is –21.0 and –19.2 kcal mol^{–1}, respectively. Clearly, the pyrene sites are much less reactive since the energy associated with the coordination of a Pt(PH₃)₂ unit to C₂–C₃ is only –7.6 kcal mol^{–1}, a value similar to that determined for the [6:5] bond in C₆₀. Also, the BSSE was calculated for these larger complexes of C₇₀ and C₈₄, giving a small range of values between 1.1 and 2.1 kcal mol^{–1}.

The Dewar–Chatt–Ducanson model is appropriate for describing the M–(η^2 -C₂) bonding.³⁶ Previous calculations have shown that the π back-donation dominates the σ donation in these complexes and, therefore, there is an electronic transfer from the metal unit to the carbon cage.¹⁷ According to the Mulliken charges, each Pt(PH₃)₂ unit coordinated to the fullerene surface transfers approximately 0.6 electron, which is located practically at the carbons linked to the metal (see Table 5). The electron transfer is similar in

(36) Dewar, M. J. S. *Bull. Soc. Chim. Fr.* **1951**, 18, C71. Chatt, J.; Duncanson, L. A. *J. Chem. Soc.* **1953**, 2939.

the three fullerene cages studied with the characteristic that the complexes with the strongest metal–fullerene bond have higher electron transfers. For instance, in the series of $(\eta^2-C_{60})\{Pt(PH_3)_2\}_n$ ($n = 1, 2, 4,$ and 6) 0.688 e are transferred from the $Pt(PH_3)_2$ unit to C_{60} in the monoaddition complex while 0.512 e are transferred/unit in the hexaaddition complex.

Conclusions

DFT calculations were performed on the series of complexes $(\eta^2-C_{60})\{Pt(PH_3)_2\}_n$ ($n = 1, 2, 4,$ and 6), $(\eta^2-C_{70})\{Pt(PH_3)_2\}$, and $(\eta^2-C_{84})\{Pt(PH_3)_2\}$ so that we could analyze the importance of the surface curvature of the fullerene in the addition of metal–ligands and the effect of the multiple addition on the binding energy (BE) between the metal and the fullerene cage. Recently, Melchor and co-workers have shown that the curvature is a prerequisite condition for bonding of atomic phosphorus to polycyclic hydrocarbons and curved graphitic surfaces.³⁷ In fullerenes the metal always coordinates to a [6:6] C–C bond because the coordination to a [6:5] site is very unfavorable. At the best level of calculation (TZP basis set for all atoms) the energy involved

in the coordination of a $Pt(PH_3)_2$ unit to a C_{60} is almost the same as that involved in the coordination of an ethylene. The BE are well reproduced if the fullerene cage is described by a mixed basis set, TZP for the carbon atoms belonging to the coordinated pyracylene and DZP for the other carbon atoms. When the number of platinum atoms attached to the fullerene cage increases, the BE decreases only slightly, which emphasizes the local nature of the metal–fullerene interaction. In the C_{70} , the most reactive site corresponds to the bond with the most pyramidalized carbon atoms in the free fullerene. It is noteworthy that the dissociation energy (DE) of the most stable monoaddition complexes of C_{70} and C_{84} is similar to that of $(\eta^2-C_{60})Pt(PH_3)_2$, but the reactivity of the distinct [6:6] C–C bonds can be quite different. Hence, for example, the addition to a pyracylene-type site in C_{84} can be more favorable than to a pyrene-type site by 15.6 kcal mol⁻¹, almost the same energy difference found between the most and the least reactive sites in C_{70} .

Acknowledgment. This work was supported by the Spanish MCyT (Grant BQU2002-04110-C02-02) and by the CIRIT of the Generalitat de Catalunya (Grant SGR01-00315).

IC048996S

(37) Melchor, S.; Dobado, J. A.; Larsson, J. A.; Greer, J. C. *J. Am. Chem. Soc.* **2003**, *125*, 2301.